VII International Conference on Computational Methods for Coupled Problems in Science and Engineering
COUPLED PROBLEMS 2017
M. Papadrakakis, E. Oñate and B. Schrefler (Eds)

TRANSMISSION AND REFLECTION OF LONG WAVES OVER STEEP BATHYMETRY VARIATIONS USING LARGE FLOATING STRIPS OF SHALLOW DRAFT

THEODOSIOS K. PAPATHANASIOU*, ANGELIKI KARPERAKI†

* Department of Mechanical, Aerospace and Civil Engineering,
Brunel University London, Uxbridge UB8 3PH, UK
e-mail: theodosios.papathanasiou@brunel.ac.uk

† School of Naval Architecture and Marine Engineering,
National Technical University of Athens, Zografos, 15773, Greece
e-mail: karperaki.ang@gmail.com

Key words: Hydroelasticity, Long Waves, Floating Breakwaters, VLFS, Finite Elements, Wave Reflection.

Abstract. The present study focuses on the determination of reflection and transmission characteristics for the coupled hydroelastic system involving a strip of large extent and shallow draft, floating over steep bathymetric variations and interacting with long waves. A parametric analysis with respect to the floating strip stiffness and the magnitude of the bathymetry variation for specific seabed profiles is conducted. This parametric study is expected to indicate optimum design characteristics, in terms of the strip flexural rigidity, for maximizing long wave reflection or transmission, depending on the specific application.

1 INTRODUCTION

Floating thin plates are commonly employed in the literature to model the response of geophysical formations, such as ice floes [1-2], as well as manmade structures such as floating breakwaters [3-4]. In applications where horizontal dimensions are significantly larger than the thickness of the structure, the hydroelastic effects are of great importance. Under wave excitation, the floating structure is expected to flex, leaving fractions of the incident wave energy to be transmitted, while a part of it is reflected and dissipated due to damping and friction [5]. The study of reflection and transmission characteristics of a coupled hydroelastic system yields valuable information for the optimal design of a floating breakwater structure, aiming in attenuating incoming wave action. Floating breakwaters are effective in sheltering marinas and harbours where the marine environment is of limited fetch [3-4]. The aim of these type of structures is to mitigate the transmitted energy as well as the transmitted, onshore wave amplitude. In the case of geophysical formations, such as ice floes, an estimation of energy transmission through an ice field allows for the prediction of collapse events when quanta of wave energy reach a potentially unstable ice shelf [1].

Regular wave reflection and transmission characteristics of a floating structure, resting on top of an inviscid and irrotational fluid layer is studied by means of linear water wave theory,

where lineariazation of the dynamic and kinematic free surface boundary condition is imposed. Notable are the works of Meylan and Squire [6] and Montiel [7] who consider the wave reflection and transmission for the case of an ice floe of constant depth, the latter catering for the Archimedian draft. The aforementioned works correlated the transmission coefficient of the energy conserving system with the incident wavelength. Additionally, Bennets et al [8] and Smith and Meylan [9] examined the effects of the plate thickness in the transmitted energy.

Typically, due to their small thickness-to-length ratio, hydroelasticity dominated floating structures are modelled under the Kirchhoff thin plate assumptions [1,10,12]. Additionally, as floating breakwaters are commonly positioned nearshore, shallow water assumptions become relevant. Sturova [10] developed an eigenfunction expansion technique for the calculation of the transient hydroelastic response of thin heterogeneous plates, while Praveen et al [11] consider the hydroelastic response of a thick elastic plate under regular long wave action. As nearshore regions are characterised by strongly variable seabed profiles, the effects of variable bathymetry must also be taken into account. In that note, Papathanasiou et al. [12] consider a higher order finite element scheme for the solution of the transient hydroelastic problem posed by a thin, elastic, heterogeneous beam floating over variable shallow bathymetry.

The present study focuses on the determination of reflection and transmission characteristics for the coupled hydroelastic system involving a strip of large extent and shallow draft, floating over steep bathymetry variations and interacting with long waves. The particular problem examined herein is of interest for the analysis and design of novel breakwaters, and the transmission of wave energy in specific areas for harvesting purposes. The treatment of the problem is performed by means of the higher order hydroelastic finite elements developed by Papathanasiou et al [12] for time domain analysis. These elements feature 5th degree Hermite polynomials for the approximation of the floating strip deflection combined with five-node Lagrange interpolation for the water velocity potential.

The Newmark method is employed for the time integration of the resulting discrete system. The reflection and transmission properties of the hydroelastic system are analysed in terms of the transmitted to reflected energy ratio, as calculated after the hydroelastic interactions have seized. A parametric analysis with respect to the floating strip stiffness and the magnitude of the bathymetry variation for specific seabed profiles is conducted. This parametric study is expected to indicate optimum design characteristics, in terms of the strip flexural rigidity, for maximizing long wave reflection or transmission, depending on the specific application. For the efficient operation of breakwaters, reflection is desired to be maximized. Inversely, for wave trapping and harvesting in shallow water regions bounded by shoals, transmission characteristics of the proposed system need to increase.

2 GOVERNING EQUATIONS

In the present section, the governing equations for a coupled hydroelastic problem regarding a thin, floating plate over shallow water bathymetry will be briefly presented. The reader is directed to relevant works in the literature for a more in depth discussion [1,10,12]. The horizontal axis x of a Cartesian coordinate system coincides with the mean water level, the vertical axis z pointed upwards. The plate is assumed to extend indefinitely in the direction vertical to the xz plane. The case of a flexible elastic strip is therefore considered.

The respective 1D domain $\Omega:(-\infty<x<\infty)$ is occupied by a layer of inviscid and irrotational fluid. The floating elastic strip is located at the 1D domain extending from $x=0$ to $x=L$. The thickness distribution of the flexible strip is $\tau(x)$ and its density ρ_p. The density of the fluid (water) is denote by ρ_w. The symbols S_0, S_1, S_2 will be used to denote the three subregions $0<x<L$, $-\infty<x<0$ and $L<0<+\infty$, respectively. The three regions will be termed 'region of hydroelastic interaction', 'region of transmission' and 'region of reflection' respectively. In S_0 the free water surface elevation $\eta(x,t)$ is assumed to coincide with the plate deflection. The velocity potential functions $\varphi_i, i=0,1,2$ will be used for the three abovementioned domains. The bathymetry in the domain of 'hydroelastic interaction' is given by $s(x)-d(x)$, where $s(x)$ is the variable depth of the seabed with respect to the undisturbed free surface and $d(x)=\rho_p\rho_w^{-1}\tau(x)$ is the plate draft (according to Archimedes principle). The semi-infinite, thin strip assumption allows for the modelling of the plate by means of the Euler-Bernoulli beam theory. For the hydrodynamic modeling, the linearized Shallow Water Equations are employed. The following non-dimensional variables are employed for the derivation of the resulting 1-D hydroelastic system

$$\tilde{x}=x/L,\ \tilde{\eta}=\eta/L,\ \tilde{t}=g^{1/2}L^{-1/2}t,\ \tilde{\varphi}_i=g^{-1/2}L^{-3/2}\varphi_i,\ \text{for } i=0,1,2.$$

Hence the non-dimensional initial-boundary value problem is written, after dropping tildes as

$$M\ddot{\eta}+\left(K\eta_{xx}\right)_{xx}+\eta+\dot{\varphi}_0=0,\ x\in S_0, \tag{1}$$

$$\dot{\eta}+(H\varphi_{0x})_x=0,\ x\in S_0, \tag{2}$$

$$\ddot{\varphi}_1-(H\varphi_{1x})_x=0,\ x\in S_1, \tag{3}$$

$$\ddot{\varphi}_2-(H\varphi_{2x})_x=0,\ x\in S_2, \tag{4}$$

with $M(x)=m(x)\rho_w^{-1}L^{-1}$, $K=D\rho_w^{-1}g^{-1}L^{-4}$, $H(x)=\left[s(x)-d(x)\right]/L$ in the 'hydroelastic interaction' region, $H(x)=s(x)/L$ outside the 'hydroelastic interaction' region and g the acceleration of gravity. The flexural rigidity of the plate is $D=E\tau^3(12(1-\nu^2))^{-1}$, where E is the Young's modulus and ν the Poisson's ratio of the plate material. The non-dimensionalised quiescence conditions at infinity are given as

$$\varphi_{1x}=0(x\to-\infty)\ \text{and}\ \varphi_{2x}=0(x\to\infty) \tag{5}$$

At the interfaces between subregions, mass and energy conservation dictated the following matching conditions

$$H(0^-)\varphi_{1x}(0^-,t)=H(0^+)\varphi_{0x}(0^+,t),\ H(1^-)\varphi_{0x}(1^-,t)=H(1^+)\varphi_{2x}(1^+,t)\ \text{and} \tag{6}$$

$$\dot{\varphi}_1(1^-,t)=\dot{\varphi}_0(1^+,t),\ \ \dot{\varphi}_0(1^-,t)=\dot{\varphi}_2(1^+,t) \tag{7}$$

For a freely floating plate, the non-dimensional boundary conditions at the edges of the plate

are

$$K\eta_{xx}\big|_{x=0} = 0\,, \quad K\eta_{xx}\big|_{x=1} = 0 \ \text{ and} \tag{8}$$

$$K\eta_{xxx}\big|_{x=0} = 0\,,\ K\eta_{xxx}\big|_{x=1} = 0\,. \tag{9}$$

The initial- boundary value problem is completed with appropriate initial conditions of the form

$$\eta_0(x,0) = \phi_0(x,0) = 0,\ x \in S_0 \tag{10}$$

$$\phi_1(x,0) = \partial_t \phi_1(x,0) = 0, \tag{11}$$

$$\phi_2(x,0) = 0,\ \partial_t \phi_2(x,0) = -G(x) \tag{12}$$

3 VARIATIONAL FORMULATION

The variational formulation of the initial-boundary value problem is derived in the present section. The procedure presented follows exactly the one adopted in [12]. Equations (13)-(16) are derived by multiplying (1)-(4) with the corresponding weight functions $v \in H^2(S_0)$, $-w_0 \in H^1(S_0)$, $w_1 \in H^1(S_1)$ and $w_2 \in H^1(S_2)$, integrating over the respective sub-regions and performing integration by parts,

$$\int_0^1 Mv\ddot{\eta}dx + \int_0^1 Kv_{xx}\eta_{xx}dx + \int_0^1 v\eta dx + \int_0^1 v\dot{\varphi}_0 dx = 0 \tag{13}$$

$$-\int_0^1 w_0\dot{\eta}dx + \int_0^1 w_{0x}H\varphi_{0x}dx - \left[w_0 H\varphi_{0x}\right]_0^1 = 0 \tag{14}$$

$$\int_{-\infty}^0 w_1\ddot{\varphi}_1 dx + \int_{-\infty}^0 w_{1x}H\varphi_{1x}dx - \left[w_1 H\varphi_{1x}\right]_{-\infty}^0 = 0 \tag{15}$$

$$\int_1^\infty w_2\ddot{\varphi}_2 dx + \int_1^\infty w_{2x}H\varphi_{2x}dx - \left[w_2 H\varphi_{2x}\right]_1^\infty = 0 \tag{16}$$

Adding, Eqs (13)-(16) and employing the farfield and interface conditions the variational problem is reformulated as,

Find $\eta(x,t)$, $\varphi_0(x,t)$, $\varphi_1(x,t)$ *and* $\varphi_2(x,t)$ *such that for every* $v \in H^2(S_0)$, $-w_0 \in H^1(S_0)$, $w_1 \in H^1(S_1)$ *and* $w_2 \in H^1(S_2)$ *it is,*

$$\begin{aligned}\int_0^1 Mv\ddot{\eta}dx + \int_0^1 v\dot{\varphi}_0 dx - \int_0^1 w_0\dot{\eta}dx + \int_{-\infty}^0 w_1\ddot{\varphi}_1 dx + \int_1^\infty w_2\ddot{\varphi}_2 dx \\ + a(\eta,v) + b_0(\varphi_0,w_0) + b_1(\varphi_1,w_1) + b_2(\varphi_2,w_2) = 0\end{aligned} \tag{17}$$

where the bilinear functionals $a(\eta,v) = \int_0^1 \left(Kv_{xx}\eta_{xx} + v\eta\right)dx$, $b_0(\varphi_0,w_0) = \int_0^1 w_{0x}H\varphi_{0x}dx$ $b_1(\varphi_1,w_1) = \int_{-\infty}^0 w_{1x}H\varphi_{1x}dx$, $b_2(\varphi_2,w_2) = \int_1^\infty w_{2x}H\varphi_{2x}dx$ have been introduced.

For the solution of the above variational problem, the finite element scheme proposed by Papathanasiou et al [12] will be adopted. In particular, we are interested for the solution of the initial boundary value problem corresponding to a long wave pulse generated in the 'transmission region', propagating and interacting with the floating plate. A part of this pulse enters the 'reflection region', while another part is reflected and back-propagates towards $+\infty$ The computational spatial domain that will be used is set such that x extends from $-x_A$ to x_B, where these values define a spatial domain large enough so that the pulses do not reach the computational domain boundaries in the examined time interval. Thus the conditions for the velocity potential spatial derivative (velocity) at infinity are also valid at the edges of the computational domain.

4 FINITE ELEMENT FORMULATION

For the free water surface subregions, that is for the 'transmission region' and the 'reflection region', finite elements with fourth order Lagrange polynomial shape function are employed. For the region of the hydroelastic coupling, a special hydroelastic element featuring quantic Hermite polynomials for the plate deflection and fourth order Lagrange shape functions for the approximation of the velocity potential is used. The reader is directed to the work of Papathanasiou *et al* [12] for a more in depth analysis. Hence, the approximate solutions in a given hydroelastic element are defined as,

$$\eta^h = \sum_{i=1}^{6} H_i(x)\eta_i^h(t) \text{ and } \varphi_j^h = \sum_{i=1}^{5} L_i(x)\varphi_{ij}^h(t), j=1,2 \tag{18}$$

Substituting the above into the discretized variation problem defined by Eq. (17) results in a second order system of the form $\mathbf{M}\partial_{tt}u + \mathbf{C}\partial_t u + \mathbf{K}u = 0$, where vector u contains the total nodal unknowns. This ordinary differential equation system has the standard form of the second order equations of structural dynamics. The implication here being each matrix is singular. The stability results in [12] however guarantee a unique solution of this discrete system. That is, an appropriate linear combination of the matrices appearing in this dynamic system must be invertible. This fact enforces the application of an implicit time integration procedure. Subsequently, a Newmark time integration scheme (see [12]) is employed in order to calculate the solution of the ordinary differential equation system. The particular values for the Newmark method $\gamma = 1/2$ and $\beta = 1/4$ have been used in all the numerical results that follow. The number of time steps employed is in all cases sufficient to ensure high accuracy.

5 NUMERICAL RESULTS

The aim of the present study is to examine the reflection and transmission properties of the aforementioned hydroelastic system, under long wave impact. In order to investigate the effect of bathymetric changes, two seabed profiles are examined. The first bathymetric profile (Figure 1) features a single peak, with the depth given by,

$$s(x) = B - b\exp\left(-50(x-x_0)\right)^2 \tag{9}$$

where x_0 is the location of the Gaussian peak. The second profile (Figure 2) features a shoaling region, where the incident wave initially propagates at constant depth B and transmits into the region of shallower constant depth b . The depth function in this case is given as,

$$s(x) = B - \frac{b}{2} + \frac{b}{2}\tanh\left(10(x - x_0)\right) \tag{20}$$

For each bathymetric profile, three different configurations are examined. In the first configuration (Configuration I), the plate is positioned in such a way that $x = 0$ is located exactly above the middle of the varying seabed interval. That is, the incoming pulse begins to interact with the plate before shoaling effects due to bathymetry variations take place. In the second configuration (Configuration II), the plate is positioned with its central point above the middle of the varying seabed region. The third case, Configuration III, involves the plate being positioned with its right hand end being over the middle of the varying topography interval. In this case, the shape of the pulse entering the hydroelastic region is affected by shoaling phenomena (see also Figures 1, 2).

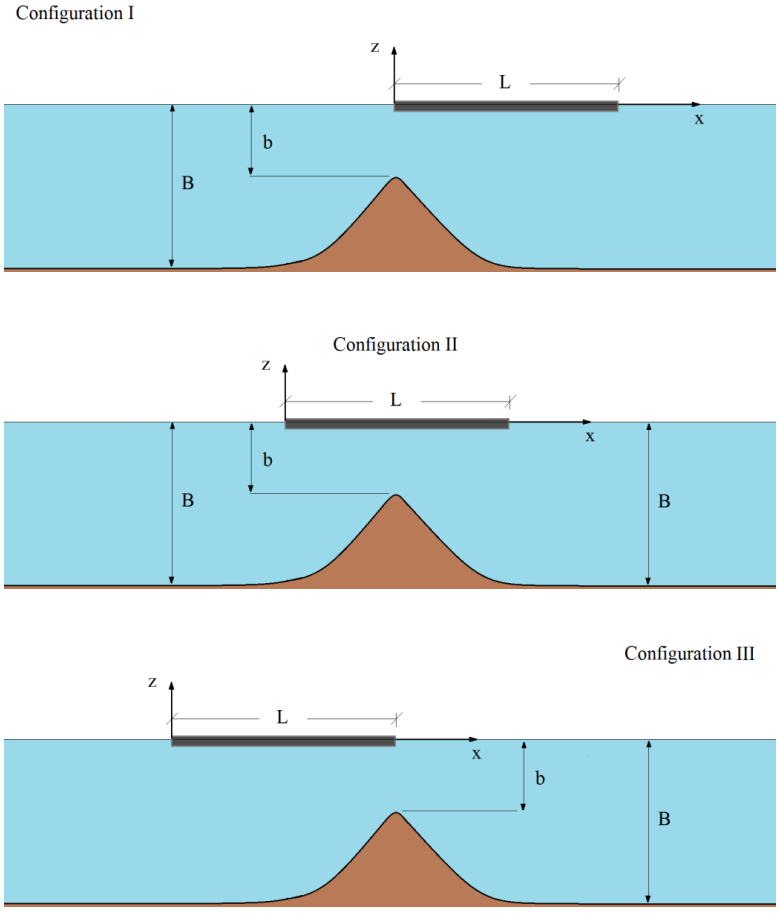

Figure 1: Schematic representations of (top) Configuration I (middle) Cnfiguration II (bottom) Configuration III described by Eq. (19)

Finally, the material constants selected are plate density $\rho_e = 900\ kg/m^3$, water density $\rho_w = 1025\ kg/m^3$, and Poisson's ratio $v = 0.3$, while a set of values for the Young's modulus is employed. The acceleration of gravity is $g = 10\ m/\sec^2$.

An initial elevation pulse of the form $\eta(x) = 2A_0 \exp\left(-\mu\left(x - x_0\right)^2\right)$, where, in the nondimensional setting, $A_0 = 3.3 \cdot 10^{-4}$ is the amplitude, x_0 is the point of origin and μ is a positive parameter controlling the smoothness of the pulse taken as 250, is allowed to propagate from location x_0 in region S_2.

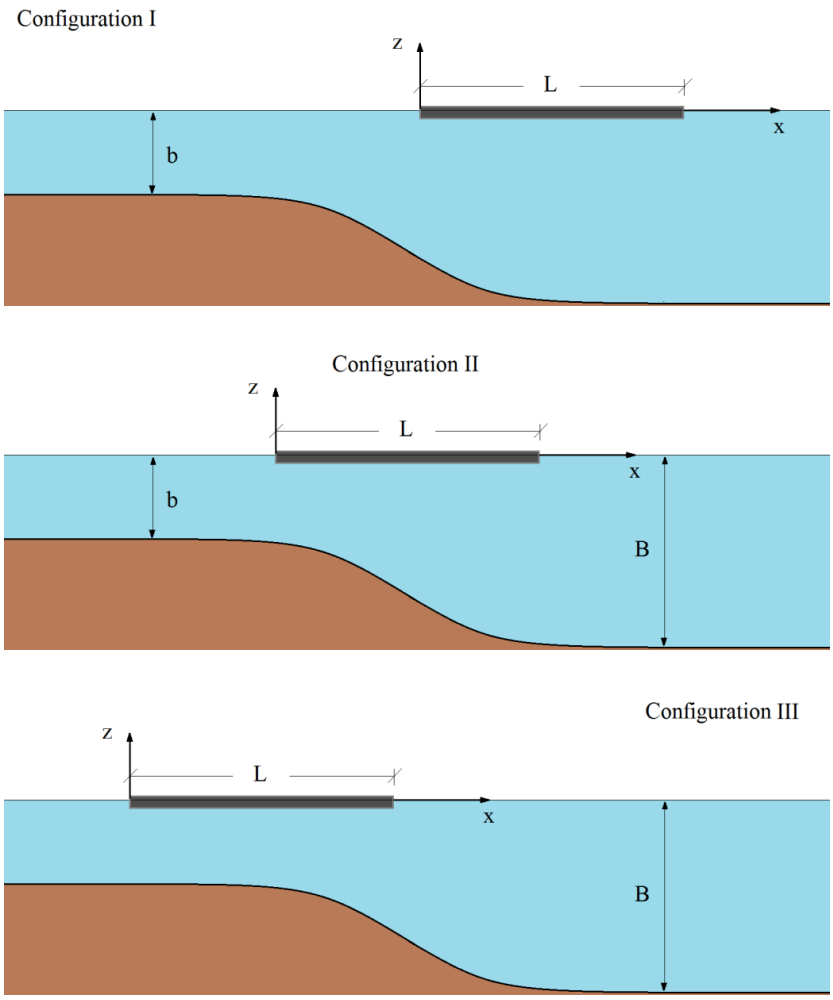

Figure 2: Schematic representations of (top) Configuration I, (middle) Configuration II, (bottom) Configuration III for bathymetric profile described by Eq. (20)

5.1 Bathymetric profile 1

The phenomenon under study involves an initial upper surface elevation disturbance that is split into two propagating waves, travelling in opposite directions, each with amplitude A_0. As the incoming wave impacts the floating plate, the excitation is partially reflected back into S_2. Figure 3 demonstrates the correlation between the ratio of energy in the region of transmission to the total energy and the natural logarithm of the nondimensional stiffness K of the floating plate, after the elastic body has reached a state of rest.

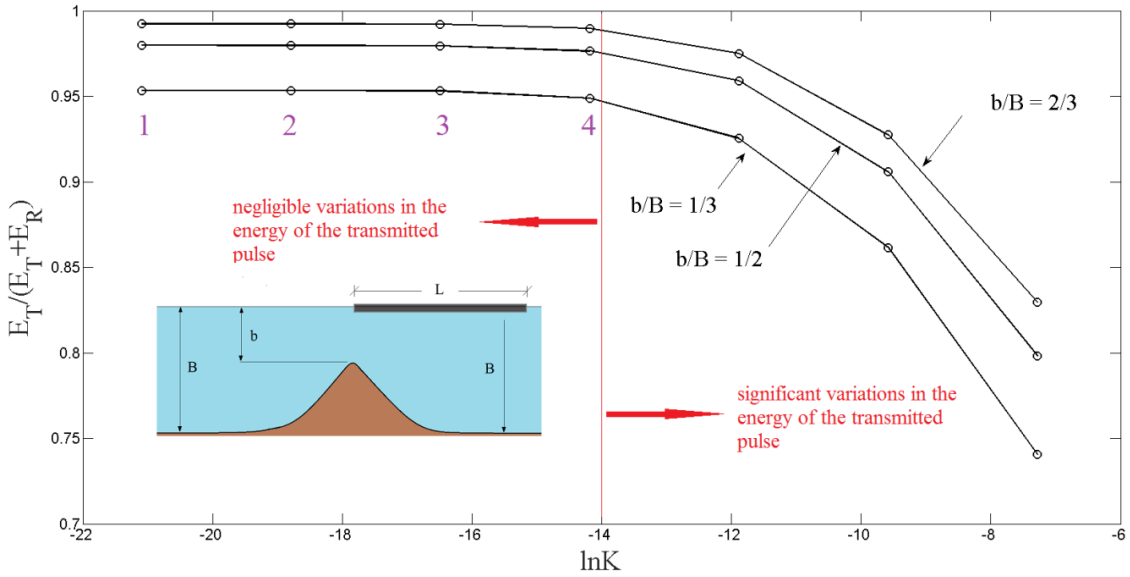

Figure 3: Ratio of the transmitted to total energy of the incoming pulse for Configuration I as a function of the natural logarithm of K. Three values for the ratio b/B have been examined.

Parameter K is derived by considering a set of values $\left(5\cdot10^{6}\sim5\cdot10^{12}\,Pa\right)$ for the Young's Modulus E. It is observed that as the local depth b at the Gaussian peak decreases, larger fractions of wave energy are reflected into S_2, manifested as a drop in the examined transmitted to total energy ratio in Fig. 3. Notably, it is seen that for the first four of the considered values for $\ln K$ (corresponding to $E=5\cdot10^{6}\sim5\cdot10^{9}\,Pa$) the variation of the ratio between the transmitted energy and the total energy is negligible for all examined d/B ratios. Points 1-4 of Fig. 3, suggest that large sums of energy are transmitted into region S_1 for the corresponding stiffness values. Figure 4 depicts the form of the transmitted wave inside region S_1, after the plate has reached a state of rest, corresponding to points 2 (left column) and 4 (right column) for $d/B=1/2$. Despite the fact that large sums of energy are transmitted, as previously shown, the peak amplitude is significantly decreased as the plate becomes stiffer. For a softer plate the incident wave pulse exhibits some hydroelastic dispersion only in the case of Configuration I. This is attributed to the location of the plate with respect to the peak, since hydroelastic interactions take place in deeper water conditions. Increasing plate stiffness successfully reduces the incident wave amplitude, generating a wavetrain in the region of transmission.

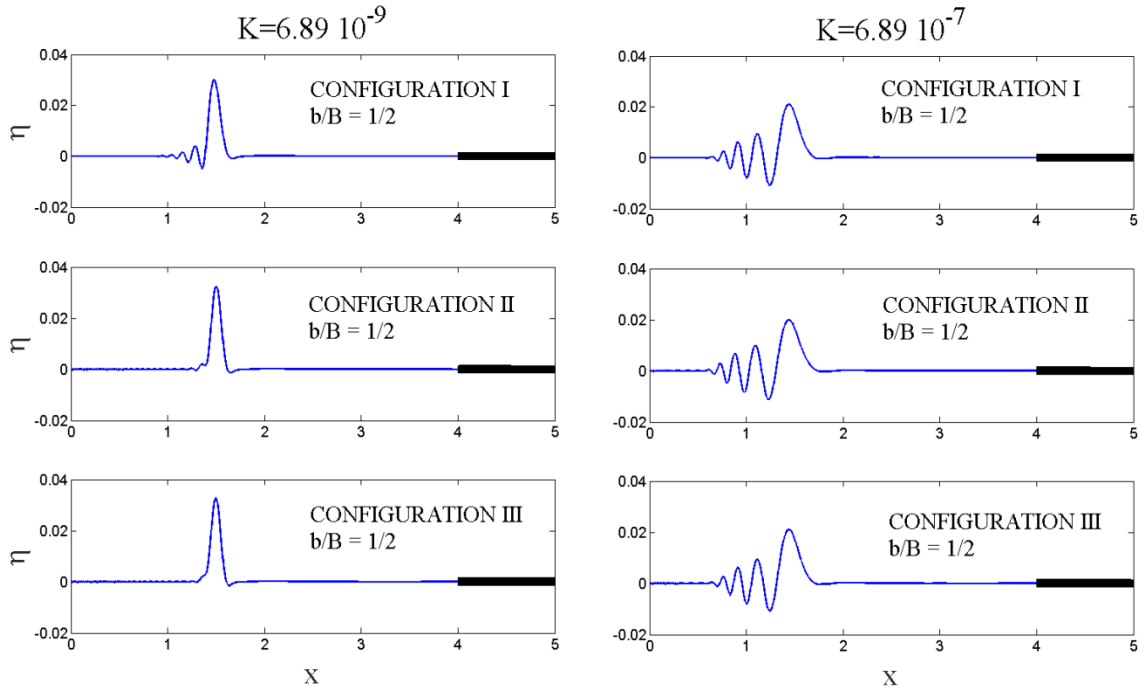

Figure 4: Form of the transmitted pulse for two cases of the plate stiffness and $b/B = 1/2$. The case of a 'soft' plate (left column) and the case of the 'stiff' plate (right hand column) correspond to approximately equal values of the transmitted energy (points 2 and 4 in Figure 3).

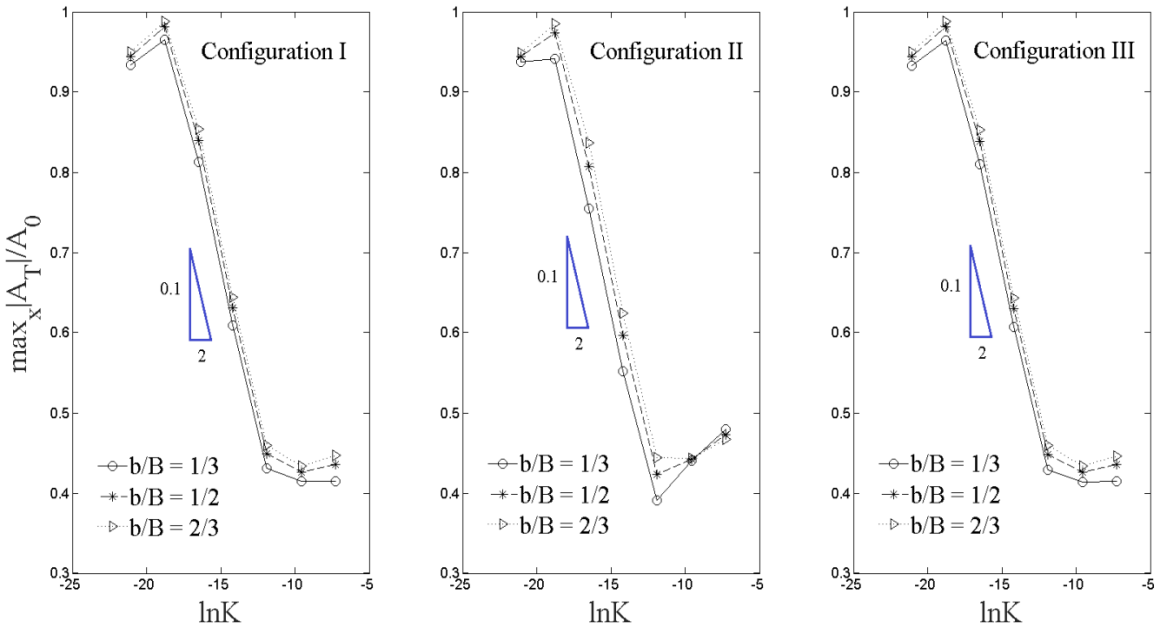

Figure 5: Ratio of the maximum amplitude of the transmitted pulse after hydroelastic interactions occur and the plate is at rest, to the amplitude of the incoming pulse, as a function of the natural logarithm of K. An almost linear decrease of the ratio for intermediate values of the stiffness is observed.

When examining the ratio of the maximum transmitted wave amplitude to the incident amplitude as a function of $\ln K$ for all three configurations and varying b/B ratios an almost linear decrease of the ratio for intermediate values of the stiffness is observed.

5.2 Bathymetric profile 2

The same analysis is applied to the second bathymetric profile featuring a shoaling region. Figure 6 shows the same approximate invariance of the ratio of transmitted to total wave energy for the first four examined values of $\ln K$. As the shallower depth b decreases, the ratio exhibits a drop once again due to larger sums of energy being reflected due to the steeper bathymetric variation.

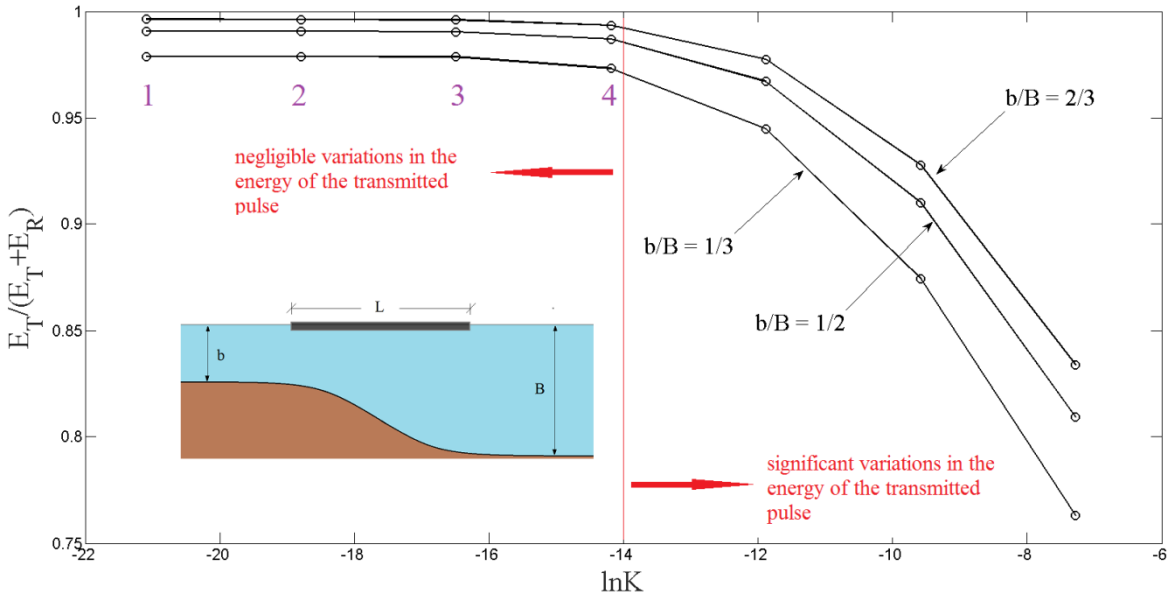

Figure 6: Ratio of the transmitted to total energy of the incoming pulse for Configuration I as a function of the natural logarithm of K. Three values for the ratio b/B have been examined.

In Fig. 7 the transmitted wave forms are again illustrated as in Fig. 4 for the second bathymetric profile. As previously observed, for a softer plate the transmitted wave form is only mildly altered. However, the amplitude of the transmitted wave for a softer plate appears increased for all three configurations. The amplitude is indeed amplified by the decreasing depth, while the stiffness of the plate appears to have minimal impact on wave attenuation. By increasing the plate stiffness the transmitted peak wave amplitude appears reduced. Once again despite the fact that the transmitted energy to total energy ratio shows no dependence upon stiffness for a range of values corresponding to points 1-4 in Fig. 6, the wave amplitude in the region of transmission appears significantly reduced for the values $\ln K$ matching points 2 and 4 (Fig.6). In Fig 8., the ratio of the maximum transmitted wave amplitude to the incident amplitude as a function of $\ln K$ is examined in a similar manner as in Fig. 5. Once again it is observed that the dependence is almost linear. For smaller stiffness values the amplitude increase due to shoaling is observed, with transmitted to incoming wave amplitude ratio increasing for decreasing b/B values.

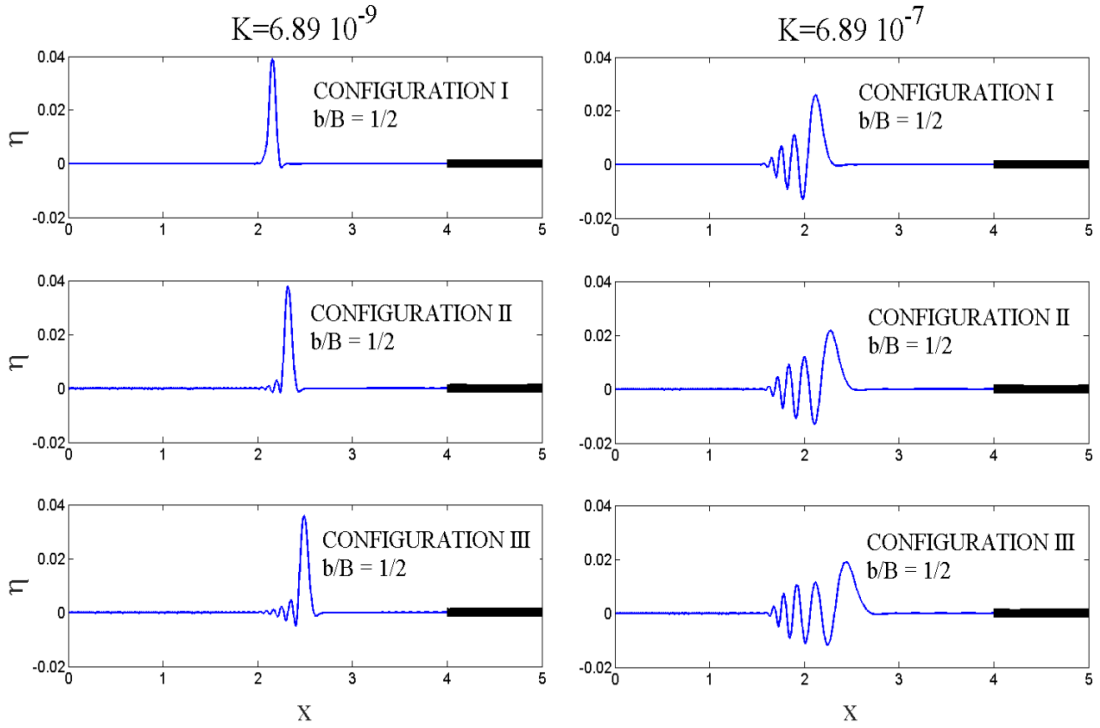

Figure 7: Form of the transmitted pulse for two cases of the plate stiffness and $b/B = 1/2$. The case of a 'soft' plate (left column) and the case of the 'stiff' plate (right hand column) correspond to approximately equal values of the transmitted energy (points 2 and 4 in Figure 6).

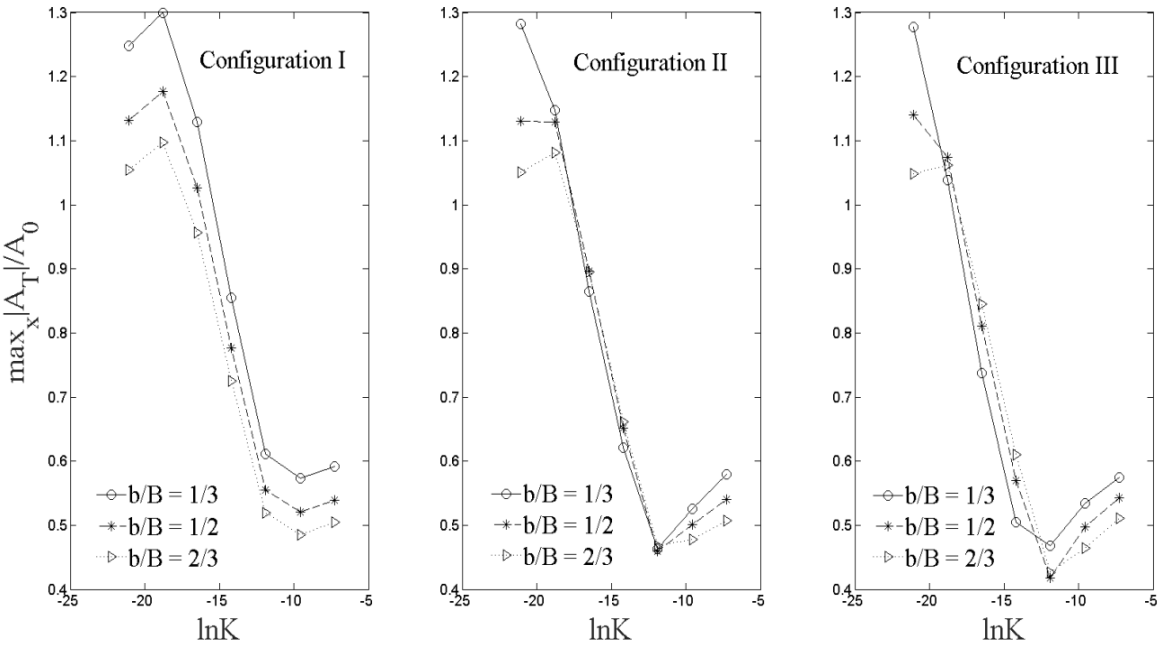

Figure 8: Ratio of the maximum amplitude of the transmitted pulse when the plate is at rest, to the amplitude of the incoming pulse, as a function of the natural logarithm of K. An almost linear decrease of the ratio for intermediate values of the stiffness is observed.

6 CONCLUSIONS

In this contribution the transmission and reflection characteristics of a floating, elastic strip over variable bathymetry, subjected to long wave impact, were examined. A parametric analysis with respect to the floating strip stiffness and seabed variations was conducted with the use of a special hydroelastic element. The ratio of transmitted to total energy, calculated at a moment in time when the plate is at rest, was seen to be independent of plate stiffness up to values reaching $E \sim 10^9 Pa$. However, despite the large calculated values for the transmitted energy, the transmitted wave amplitude was significantly reduced. At the same time, the transmitted pulse features dispersion due to hydroelastic phenomena. This result illustrates the fitness of the examined configurations for wave attenuating applications.

REFERENCES

[1] Papathanasiou, T.K., Karperaki, A.E., Theotokoglou, E.E. and Belibassakis, K.A. Hydroelastic analysis of ice shelves under long wave excitation, *Nat. Hazards Earth Syst. Sci*., (2015), **15**: 1821-1857.

[2] Squire, V.A. Synergies between VLFS Hydroelasticity and Sea Ice Reasearch, *Int. J. offshore polar,* (2008), **18** (3):1-13.

[3] Wang, C.M. and Tay, Z.Y. Very Large Floating Structures: Applications, Research and Development, *Proc. Engineering*, **14**: 62-72

[4] Wang, C.M., Watanabe E. and Utsunomiya, T. *Very large floating structures*, Taylor and Francis, London, (2008).

[5] Koutandos, E., Prinos, P. and Gironella, X. Floating breakwaters under regular and irregular wave forcing: reflection and transmission characteristics, *J. Hydraul. Res.* (2005), Vol 43 **(2)**:174-188.

[6] Meylan, M.H. and Squire, V.A. The response of ice floes to ocean waves, *J. Geopysh Res* (1994) **99** (C1):891-900

[7] Montiel, F., Bennetts L.G. and Squire, V.A. The transient response of floating elastic plates to wavemaker forcing in two dimensions, *J. Fluids Struct.* (2012) **28**: 416–433.

[8] Bennetts, L.G., Biggs, N.R.T. and Porter, D. A multi-mode approximation to wave scattering by ice sheets of varying thickness, *J. Fluid Mech.* (2007) **579**: 413-443.

[9] Smith, M.J.A. and Meylan, M.H. Wave scattering by an ice floe of variable thickness, *Cold Reg. Sci. Technol*. (2011) **67** (1–2): 24–30.

[10] Sturova, I.V. Time-dependent response of a heterogeneous elastic plate floating on shallow water of variable depth. *J. Fluid Mech.* (2009), **637**:305-325.

[11] Praveen, K.M, Karmakar, D. and Nasar, T. Hydroelastic analysis of floating elastic thick plate in shallow water depth, *Perspect. in Sci.* (2016), **8**: 770-772

[12] Papathanasiou, T. K, Karperaki, A., Theotokoglou E.E. and Belibassakis, K.A.. A higher order FEM for time-domain hydroelastic analysis of large floating bodies in an inhomogeneous shallow water environment, *Proc. R. Soc. A*, **471**: 20140643, (2014).